from $\Delta M_{\max}$, provided $\Delta M_{\max}$ may be found to 10%, which is conservative.

Using M_{T2} it is possible to measure $\Delta M_{\max} = m_{\tilde{l}} - m_{\tilde{\chi}_1^0}$ to 10% or better.

Endpoint	S5 Fit	S5 Fit error	O1 Fit	O1 Fit error	Table 4 values S5	Table 4 values O1
l^+l^- edge	109.10	0.13	70.47	0.15	109.12	70.50
l^+l^-q edge	532.1	3.2	544.1	4.0	536.7	530.5
$l^{\pm}q$ high-edge	473.4	5.9	482.3	10.5	464.2	513.6
$l^{\pm}q$ low-edge	317.0	4.7	243.1	3.6	399.1	231.2
l^+l^-q threshold	266.0	6.4	182.2	13.5	264.9	168.1
Xq edge	514.1	6.6	525.5	4.8	509.2	503.4
ΔM (M_{T2} edge)	——	——	——	10%	35.7	92.5

Table 6: Endpoints and associated fit uncertainties. The results of the naive fits shown in Figures 5 and 6 may be seen in the 'fit' and (one-sigma) 'fit error' columns. For the reasons outlined in Section 3.1 there is presently a lack of good theoretical predictions for these edge postions. (In this context a "good prediction" is one capable of taking into account, up to a level compatible with the statistical/fit errors, either the naivety of the fits, or the effects introduced by edge distortions and the presence of backgrounds.) The best guides presently available are the quantities listed in Table 4, evaluated at $m_{\tilde{q}}$ equal to the largest squark mass. These values are also shown for comparison purposes. All values are GeV except where stated otherwise.

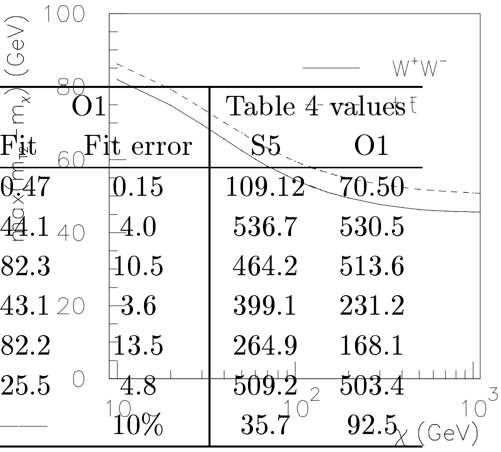

Figure 10: Variation with χ of the SM contributions to $\max(M_{T2}(\chi) - \chi)$ (for a number of events corresponding to 100 fb^{-1}) which provides a measure of the minimum $\tilde{l}$-$\tilde{\chi}_1^0$ mass difference which is needed for signal M_{T2} events to be able to extend beyond the SM backgrounds. Events contributing to this plot were selected using the "hard" M_{T2} cuts.

3.6 Reconstructing sparticle masses

Sparticle masses are reconstructed by performing a chi-squared fit with between four and six free parameters p. The main parameters of the fit are $m_{\tilde{\chi}_1^0}$, $m_{\tilde{l}}$, $m_{\tilde{\chi}_2^0}$ and $m_{\tilde{q}}$. Where appropriate, m_h and m_Z also appear as fit parameters, although if they do, they are strongly constrained (particularly in the case of the Z) by present LEP measurements or expected LHC errors (0.0077% and 2.0% respectively).

The chi-squared, as a function of the free parameters p, is then formulated as:

$$\chi^2(p) = \sum_1^n \frac{(O_i^{\rm sm} - O_i(p))^2}{{\sigma_i}^2}, \qquad (3.7)$$

where $O_i^{\rm sm} = O_i(p_{\rm model}) + \sigma_i X_i$ are n "smeared observables", $X_i \sim N(0,1)$ are the n random variables from the Normal distribution (with mean 0 and standard deviation 1) which accomplish the smearing, σ_i is the anticipated statistical error for the $i^{\rm th}$ observable (approximated by the fit error listed in Table 6), and $O_i(p)$ is the value one would expect for the $i^{\rm th}$ observable given the parameters p (for examples see Table 4). $p_{\rm model}$ indicates the actual masses of the sparticles in the particular model being considered. The results of the fit, $p_{\rm fit}$, are then those which minimise the chi-squared. $p_{\rm fit}$ may be interpreted as the sparticle masses which might be reconstructed by an LHC experiment after obtaining 100fb^{-1} at high luminosity, with the X_i parametrising the experimental errors. Since it is clearly desirable to know the accuracy with which this reconstruction can be performed, the above fitting process is repeated many times for different values of the X_i, and the